Methylammonium Lead Chloride: A Sensitive Sample for an Accurate NMR Thermometer

Guy M. Bernard, Atul Goyal, Mark Miskolzie, Ryan McKay, Qichao Wu,

Roderick E. Wasylishen* and Vladimir K. Michaelis*

Department of Chemistry, University of Alberta, Edmonton AB T6G 2G2 Canada

* Corresponding authors: vladimir.michaelis@ualberta.ca

roderick.wasylishen@ualberta.ca

Keywords: NMR thermometry; IUPAC; internal reference; ^{207}Pb MAS NMR spectroscopy; frictional heating; $MAPbCl_3$

Abstract

A new solid-state nuclear magnetic resonance (NMR) thermometry sample is proposed. The ^{207}Pb NMR chemical shift of a lead halide perovskite, methylammonium lead chloride ($MAPbCl_3$) is very sensitive to temperature, 0.905 ± 0.010 ppm·K^{-1}. The response to temperature is linear over a wide temperature range, from its tetragonal to cubic phase transition at 178 K to > 410 K, making it an ideal standard for temperature calibrations in this range. Because the ^{207}Pb NMR lineshape for $MAPbCl_3$ appears symmetric, the sample is ideal for calibration of variable temperature NMR data acquired for spinning or non-spinning samples. A frequency-ratio method is proposed for referencing ^{207}Pb chemical shifts, based on the ^{1}H and ^{13}C frequencies of the methylammonium cation, which are used as an internal standard. Finally, this new NMR thermometer has been used to measure the degree of frictional heating as a function of spinning frequency for a series of MAS rotors ranging in outer diameter from 1.3 to 7.0 mm. As expected, the largest diameter rotors are more susceptible to frictional heating, but lower diameter rotors are subjected to higher frictional heating temperatures as they are typically spun at much higher spinning frequencies.

1. Introduction

Variable-temperature (VT) nuclear magnetic resonance (NMR) spectroscopy is routinely used to study the thermodynamic and kinetic properties of solutions[1] and solids.[2–4] These investigations critically depend on precise knowledge of the temperature experienced by the sample. Unfortunately, experimental and hardware limitations mean that one cannot assume that the temperature set by the instrument's temperature controller is the actual temperature experienced by the sample. For example, hardware required for magic-angle spinning (MAS) requires that the temperature sensor be placed at some distance from the sample; this concern is not limited to MAS experiments since NMR spectra of non-spinning samples are often acquired with MAS probes. Solution[5,6] and imaging[7] NMR spectroscopists often experience similar challenges, *e.g.*, local thermal gradients in or near the probe head for cryogenically cooled probes.[8] Radio-frequency irradiation can lead to sample heating (*e.g.*, long decoupling, or high-power spinlocking) particularly for solid biological samples,[9,10] but often in solid-state NMR a more immediate consideration is frictional heating resulting from the drive and bearing gases typically introduced at ambient temperatures during MAS experiments. This effect is not necessarily uniform,[11] becoming a particular concern as MAS technology evolves to higher spinning frequencies (*i.e.*, 60 to 120 kHz) and beyond.[12] In addition, hardware constraints often prevent a uniform distribution of the VT gas stream over the sample volume, potentially leading to additional temperature gradients.

To accurately determine temperatures experienced by samples under investigation in NMR probes, numerous compounds have been proposed as "NMR thermometers".[13] Probably the preferred method is to calibrate the temperatures reported by the controller software through the use of chemical shift thermometers. For samples in solution, these have often been calibrated

based on the chemical shift differences between the aliphatic and hydrogen-bonded hydroxyl ^{1}H nuclei of ethylene glycol (303.4 K < T < 372.4 K) or methanol (238.8 K < T < 308.8 K).[14] The sensitivity of paramagnetic Fe(II) and Co(II) shift agents to temperature has also been used as an NMR thermometer for samples in solution.[15] For solid samples, the ^{207}Pb chemical shift of lead nitrate has commonly been used to calibrate the sample temperature.[11,16–22] At cryogenic temperatures, such as those required for dynamic nuclear polarization (DNP) NMR spectroscopy, careful calibration of the temperature with neoptix sensors is common;[23] the same goal is sometimes achieved by tracking the ^{79}Br chemical shift or nuclear spin-lattice relaxation (*i.e.*, T_1) of KBr.[24] For temperatures in the mK range, population difference thermometry has been used.[25] Generally, external standards have been used for temperature calibrations in solid-state NMR, but Pan and Gerstein[26] suggested the temperature dependence of the ^{31}P NMR signal of $(VO)_2P_2O_7$ as an internal standard, since ^{31}P is a sensitive nucleus whose signal does not interfere with those of commonly observed solid-state NMR nuclei, such as ^{13}C or ^{29}Si. A complete summary of NMR techniques used to measure experimental temperatures is beyond the scope of this introduction; see Table 1 for a list of NMR thermometers proposed over the past two decades and Supporting Information (SI) for a more detailed report on the methods presented in this table.

Table 1. Selected Examples of Solid-State NMR Thermometers[a]

Sample	Nucleus	Method	Reference
TTMSS[b]	^{1}H	Chemical shift	27
$Li_{0.24}La_{0.54}TiO_3$	^{7}Li	T_1	28
TmDOTA[c]	^{13}C	Chemical shift	29
various[d]	^{13}C	Phase transitions	30
$(VO)_2P_2O_7$	^{31}P	Inverse chemical shift	26
CuBr	^{63}Cu	Chemical shift	31
CuI	^{63}Cu	Chemical shift	31
KBr	^{79}Br	Chemical shift and T_1	24,32
$Sm_2Sn_2O_7$	^{119}Sn	Inverse chemical shift	16,33−35
$Nd_2Sn_2O_7$	^{119}Sn	Inverse chemical shift	34
CsI	^{127}I	T_1	36
$Pb(NO_3)_2$	^{207}Pb	Chemical shift	11,16−22

a see Supporting Information for more details on these and other NMR thermometers.
b TTMSS = tetrakis(trimethylsilyl)silane.
c TmDOTA = thulium-1,4,7,10-tetraazacyclododecane-1,4,7,10-tetraacetate.
d adamantane, *d*-camphor, pivalic acid and 1,4-diazo[2.2.2]octane (DABCO).

The NMR thermometers presented in Table 1 and in the supporting information demonstrate that a "one size fits all" solution to NMR thermometry has not been found. One reason for this is the versatility of NMR spectroscopy; investigators often acquire NMR data at very low or very high temperatures and suitable samples do not cover the entire temperature range. For example, while T_1(^{79}Br) for KBr is sensitive to temperatures at least as low as 20 K,[24] the T_1 values at very low temperatures are on the order of minutes, rendering the technique impractical. In addition, at temperatures above 100 K, measured ^{79}Br T_1 values for KBr are also sensitive to field strength and experimental setup which may lead to significant discrepancies in estimated temperatures;[37] the ^{79}Br chemical shift for this sample is sensitive to temperature, but the linearity between chemical shifts and temperature breaks down for temperatures below 100 K. Tekely and coworkers also recommend using the ^{79}Br chemical shift of KBr as an NMR thermometer, but suggest that magnet stability be monitored through the acquisition of ^{13}C spectra of adamantane in a mixture of the two samples; the chemical shifts of the latter are insensitive to temperature, so

variations in ^{13}C chemical shifts are an indication of magnet instability.[32] Because of the inverse temperature dependence of the ^{119}Sn chemical shifts for paramagnetic $Sm_2Sn_2O_7$ or $Nd_2Sn_2O_7$, NMR thermometers based on these complexes are more sensitive at lower temperatures.[33–35]

In the course of our investigations of methylammonium lead halide perovskites ($MAPbX_3$, X = Cl, Br, I),[38–40] we became aware of a strong temperature dependence of the ^{207}Pb chemical shift for $MAPbCl_3$. The sample is easily prepared, stable over a wide temperature range, and exists in the cubic phase from 178 K[39,41] up to its decomposition (~ 450 K).[42] Its structure has been determined by several investigators;[39,43–47] all report similar structures when the sample is in the cubic phase and there have been no reports of polymporphism. Since the ^{207}Pb nuclei are at sites of octahedral symmetry when the sample is in the cubic phase,[39,41] they are not subject to anisotropic magnetic shielding, yielding ^{207}Pb NMR peaks that for practical purposes are symmetric at moderate magnetic fields, albeit broadened significantly (*vide infra*).

Calibrating variable temperature NMR data obtained for non-spinning samples can be challenging, since the calibration standards (*e.g.*, $Pb(NO_3)_2$) yield asymmetric powder patterns due to anisotropic magnetic shielding, complicating the analysis of the data. Nevertheless, Beckmann and Dybowski proposed a chemical shift thermometer for non-spinning samples based on the sensitivity of the most intense component of the powder pattern observed for $Pb(NO_3)_2$ at a given temperature.[18] As discussed below, $Pb(NO_3)_2$(aq) yields a single isotropic peak, but unfortunately the chemical shift in this case is not only sensitive to temperature, but also to concentration[48] and solvent.[49] Hence, a solid-state temperature calibration standard that is very sensitive to temperature and that yields symmetric peaks for non-spinning samples is highly desirable. We have therefore undertaken a VT NMR investigation of the temperature dependence of the ^{207}Pb NMR chemical shift of $MAPbCl_3$, with the goal of establishing a new solid sample

as an NMR standard for the calibration of temperatures obtained for NMR spectra of non-spinning samples; of course the method is also useful for measuring the temperature of spinning samples. Because MAS is not required, the sample is also effective for temperature calibrations in solution or non-spinning NMR probes, and may become a useful addition to established IUPAC temperature reference standards. We show that the ^{207}Pb chemical shift scale may be derived through the determination of the ^{1}H or ^{13}C frequencies of the methylammonium ion of $MAPbCl_3$, avoiding errors inherent in setting the reference scale on the basis of the chemical shift of temperature-sensitive Pb-containing samples and thus providing a reliable absolute temperature thermometer. As an alternative, we demonstrate that the temperature can be derived independent of chemical shift, based solely on the relationship between the resonant frequencies of ^{13}C or ^{1}H and of ^{207}Pb.

2. Experimental Details

Sample Preparation

$MAPbCl_3$ was prepared following the procedure outlined by Knop et al.;[39] that procedure was based on the method Weber[50] used to prepare $MAPbBr_3$. **Note**: $MAPbCl_3$ may be obtained from the authors.

Data Acquisition

Pb-207 NMR spectra of non-spinning and MAS samples were acquired on: Bruker Avance 300, Bruker Avance III HD 400, Varian Inova 400, Bruker Avance 500, Agilent VNMRS 600, and Avance II 900 NMR spectrometers with a variety of probes. Spectra of non-spinning or MAS samples were acquired, without ^{1}H decoupling, with a Bloch decay. NMR rotors (either 1.3, 2.5, 3.2, 4.0 or 7.0 mm outer diameter) were fully packed with the sample; as seen below, the sensitivity was such that adequate spectra could be obtained in a few minutes (*i.e.,* 256

transients) with as little as ≈ 7 mg of sample packed into the 1.3 mm rotor. As shown below and in greater detail in SI, the ^{207}Pb NMR chemical shift scale was calibrated internally to the recommended standard (*i.e.*, $\delta_{iso}(^{207}Pb) = 0$ for $Pb(CH_3)_4$) based on either the ^{1}H or ^{13}C frequencies of the methylammonium cation of $MAPbCl_3$. Chemical shifts were determined by fitting the experimental spectra using WSolids[51] or SpinWorks.[52] Table S1 further summarizes the experimental conditions.

VT NMR measurements were undertaken on the Bruker Avance 500 NMR spectrometer, using the BVT 3000 VT unit provided by Bruker Biospin. Dry air was used for measurements in the 250 to 350 K range, while N_2(g), obtained from the boil-off N_2(l), was used at other temperatures; the flow rate ranged from 500 to 1070 L/h. The heat exchanger source was N_2(l) for temperatures below 250 K and an ethanol/dry ice bath for temperatures in the 250 K to ambient temperature range.

^{1}H MAS NMR spectra of $MAPbCl_3$ were obtained at 11.75 T on a Bruker Avance 500 NMR spectrometer with the sample spinning at frequencies ranging from 3.0 to 12.0 kHz. A Bloch pulse with a 4.0 μs 90° pulse and a 60 s recycle delay were used to acquire these spectra. ^{13}C NMR spectra were also acquired on this instrument with cross polarization and spinning frequencies ranging from 3.0 to 5.0 kHz. A 5.0 ms contact time, a 4.0 μs ^{1}H 90° pulse and a recycle delay of 60 s were used to acquire the ^{13}C NMR spectra.

Temperature Calibration

Temperature calibration was undertaken on an INOVA 400 NMR spectrometer. Variable-temperature NMR data were acquired in approximately 10 K increments between 183 and 303 K, and in approximately 20 K increments between 303 and 413 K. Three measurements were

made at each temperature: (i) the temperature as recorded with a copper/constantan thermocouple placed within the NMR tube in the region where one typically places the solution for NMR measurements; (ii) a ^{1}H NMR spectrum of ethylene glycol ($T \geq 303$ K) or methanol ($T < 303$ K); and (iii) a ^{207}Pb NMR spectrum of solid $MAPbCl_3$. The same NMR probe, with the sample or thermocouple placed in a 5 mm solution NMR tube, were used for these measurements. Samples were swapped at each VT point, allowed to thermally equilibrate (≈ 20 minutes), followed by acquisition of the experimental data point. Dry $N_2(g)$ was used as the VT gas for temperatures below 233 K (or above 350 K), with the house air supplying the VT gas at other temperatures. The heat exchanger source for temperatures below ambient was $N_2(l)$ ($T <$ 233 K) or an ethanol/dry ice bath for the 233 K to ambient temperature range. For ^{1}H NMR measurements of ethylene glycol or methanol, temperatures were calculated based on the relationship between the hydroxyl and aliphatic ^{1}H chemical shifts as reported by Raiford and coworkers.[14] As discussed below, temperatures obtained from this procedure yielded virtually identical results with those obtained from the copper/constantan thermocouple. Unless otherwise specified, temperatures reported here were obtained from the copper/constantan thermocouple or from the ^{207}Pb chemical shifts of $MAPbCl_3$ and their temperature dependence as determined from these measurements.

3. Results and Discussion

Temperature Calibration

Fig. 1 illustrates ^{207}Pb NMR spectra of solid $MAPbCl_3$ acquired at 9.39 T at various temperatures. The peak widths (full width half maximum or FWHM) range from 2.9 to 3.6 kHz, with spectra obtained at lower temperatures having a greater linewidth; the source of the broadening is attributed to spin-spin interactions with six directly bonded ^{35}Cl (I = 3/2, Ξ = 9.798 %, NA = 75.78 %) and ^{37}Cl (I = 3/2, Ξ = 8.156 %, NA = 24.22 %) nuclei. Because the chlorine nuclei have nuclear quadrupole coupling constants on the order of 16 MHz,[44] the lineshape is complicated,[53] but for practical purposes symmetric for the magnetic field strengths typically used in modern NMR labs. Below 178 K, $MAPbCl_3$ undergoes a reversible transition from the cubic to the tetragonal phase[39,41] and ^{207}Pb is no longer at a site of cubic symmetry, resulting in a complicated NMR powder pattern. Although the temperature dependence of ^{207}Pb chemical shifts has been well documented,[22] the range of chemical shifts illustrated in Fig. 1 prompted a more careful examination of this phenomenon. In addition, the symmetric peaks obtained at the field strengths (7 to 21 T) used here, rarely observed for NMR spectra of non-spinning solid samples, make this sample particularly suitable for temperature calibrations involving non-spinning samples.

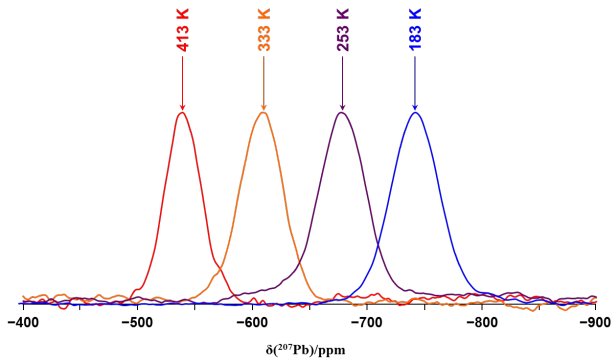

Figure 1. ^{207}Pb NMR spectra of a non-spinning solid sample of $MAPbCl_3$ acquired at 9.39 T for the temperatures indicated.

To further evaluate the temperature dependence of the ^{207}Pb chemical shifts for $MAPbCl_3$, spectra were acquired from 183 to 413 K. Fig. 2 illustrates $\delta(^{207}Pb)$ plotted as a function of the temperature obtained from the thermocouple measurement immediately prior to data acquisition. As seen in this figure, $\delta(^{207}Pb)$ is linearly dependent on temperature in the range studied here; it was fit to a linear equation of the type $\delta(^{207}Pb) = aT + b$, yielding Equation 1, with $R^2 = 0.9996$ and with a root-mean-square error of 1.2. Based on a 95 % confidence interval, the temperature dependence of $\delta(^{207}Pb)$ for $MAPbCl_3$ is 0.905 ± 0.010 ppm·K^{-1}.

$$\delta(^{207}Pb) = 0.905 \cdot T - 909.1 \qquad 1$$

Eq. 1 may be rearranged such that, if the ^{207}Pb spectra are referenced according to the protocol outlined below, one may obtain the temperature according to Eq. 2:

$$T/K = \frac{\delta(^{207}Pb) + 909.1}{0.905} \qquad 2$$

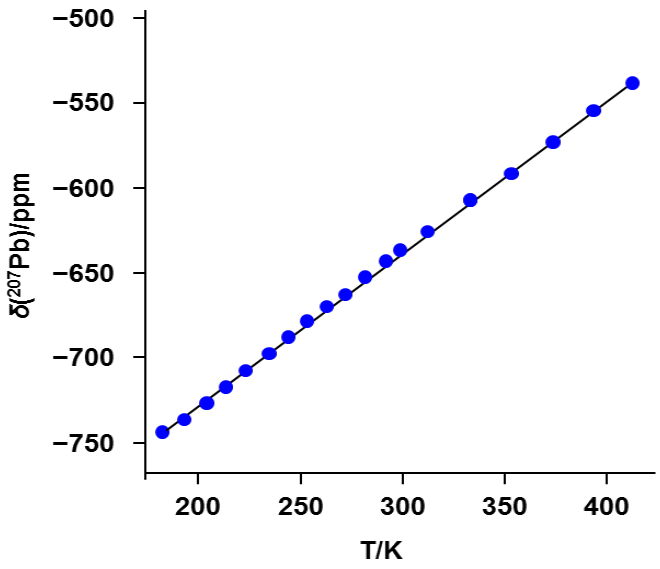

Figure 2. ^{207}Pb chemical shifts for $MAPbCl_3$ plotted as a function of temperature. Spectra were acquired on non-spinning samples at 9.39 T.

As a secondary check on the thermocouple temperature, the temperature was also obtained on the basis of the chemical shift difference between the aliphatic and hydroxyl ^{1}H nuclei of either ethylene glycol or methanol NMR standard samples; spectra of these were acquired immediately following the acquisition of the ^{207}Pb NMR spectra. As seen in Figure S1, the temperature dependence of the ^{207}Pb peaks for $MAPbCl_3$ is, within error, identical to that shown in Figure 2. Indeed, the temperature measured with the glycol/methanol standards plotted vs the temperature measured with the thermocouple (Fig. S2) yields a slope of 1.0009 and $R^2 = 0.9997$. Unfortunately, the precision achieved with the ethylene glycol or methanol standards using a solution NMR probe cannot easily be replicated when using solid-state NMR probes, emphasizing the necessity for a reliable solid-state NMR thermometer sample.

NMR spectra of non-spinning samples were also acquired at 11.75 T on a wide-bore solid-state NMR instrument; Figure 3 illustrates the chemical shifts obtained as a function of the calibrated temperatures as well as by the set temperature, serving as a reminder of the importance

of calibration when undertaking VT NMR measurements. Although a good linear relationship is obtained if the set temperature is used (R^2 = 0.9996), relying on the instrument's temperature setting results in significant errors, particularly at elevated temperatures. Note that the deviation between set and actual temperatures depends on numerous factors, such as the hardware and experimental conditions, so it is important that this calibration be done under the same conditions as used for the sample of interest. For example, the gas flow rate for the VT gas should be recorded and calibration data obtained under these conditions.

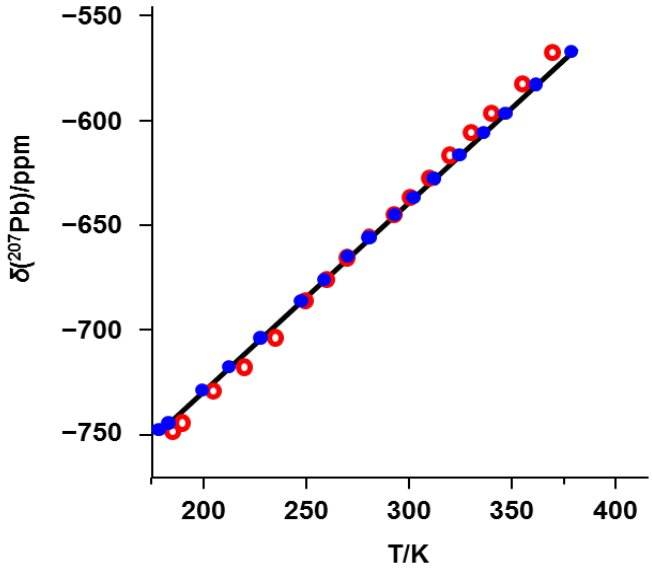

Figure 3. δ(^{207}Pb) for $MAPbCl_3$ plotted as a function of temperature. The blue closed circles and the line represent temperature values derived from Eq. 2 and the red open circles represent the temperature set by the controller software.

Frictional Heating

A concern when undertaking NMR measurements on temperature-sensitive samples is the effect of frictional heating.[11] Fig. 4 illustrates plots of the relative temperature, determined based on the chemical shift and Eq. 2, as a function of spinning frequency for MAS probes with outer diameters ranging from 1.3 to 7.0 mm. As expected, in all cases the temperature increases with

spinning frequency, with the larger diameter rotors being more sensitive. In their investigation of the effect of MAS on sample temperature for a 2.5 mm probe, Langer *et al.* found a 30 to 40 K increase in temperature when spinning samples at 35 kHz,[35] slightly less than what we observed. With the exception of the 1.3 mm rotors spinning at high frequencies (discussed below), there were no indications of temperature gradients within these rotors in these measurements. For example, a ^{207}Pb NMR spectrum of $MAPbCl_3$ obtained at room temperature with a 4 mm probe at a spinning frequency of 14 kHz yields a Gaussian peak (see Fig. S3). This suggests that the temperature within the sample does not vary by more than 2 K, since greater variations will induce a greater than 1 ppm asymmetric broadening of the peak, which would be detectable. Likewise, in their investigation of frictional heating within a 7.0 mm rotor, Grey *et al.*[34] concluded that heating within the rotor due to MAS was uniformly distributed. As noted by van Gorkom *et al.*, bearing gases are a key contributor to frictional heating,[11] but the actual pressures used for a given sample depends on conditions, such as the mass and distribution of the sample, that are not constant. External conditions, such as the quality of the rotor and of its cap, also affect the balance of drive and bearing gas pressures required to achieve stable sample spinning. In addition, changing probe designs (*e.g.*, narrow-bore probes, separate VT gas streams, *etc.*) as well as sample composition (*e.g.,* density, dielectric properties, *etc.*) mean that the response to MAS will further vary. Thus, the trends discussed in this section and illustrated in Fig. 4 should be considered general.

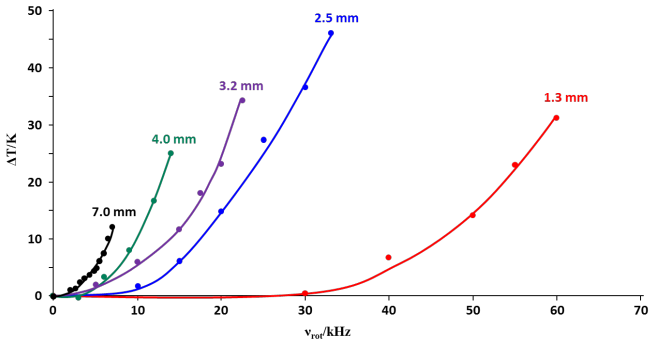

Figure 4. Plot of sample temperature as a function of spinning frequency, for the indicated rotor size (outer diameter). ^{207}Pb NMR spectra were acquired at 9.4 T (3.2 mm rotor), 11.75 T (2.5, 4.0 and 7.0 mm rotors) and 21.1 T (1.3 mm rotor) at 293 ± 1 K. ΔT indicates changes from this temperature due to frictional heating. All samples were fully packed with ground $MAPbCl_3$ in zirconia rotors with either Kel-F® or Vespel® caps.

As discussed above, frictional heating may be non-uniform.[11] Fig. 5 illustrates a series of ^{207}Pb NMR spectra acquired at 21.1 T with a 1.3 mm MAS probe at various spinning frequencies. Spinning the sample at 30 kHz has a negligible effect on δ_{iso}, indicating minimal frictional heating with these small NMR rotors at this spinning frequency. However, heating clearly becomes significant at higher spinning frequencies; at ν_{rot} = 60 kHz, the temperature within the rotor has increased by more than 30 K (clearly it is increasing exponentially with spinning frequency and is expected to exceed 40 K between 65 and 70 kHz). This is an important consideration for NMR studies of temperature-sensitive samples, such as biomolecules or paramagnetic conductive materials. The linewidths of these peaks are also informative. At ν_{rot} = 0, the ^{207}Pb NMR peak is broadened compared to that obtained for ν_{rot} = 30 or 40 kHz, reflecting the fact that MAS reduces the direct ^{207}Pb-$^{37/35}$Cl and ^{207}Pb-^{1}H dipolar interactions. However, as ν_{rot} is increased to spinning frequencies greater than 40 kHz, the peak is broadened compared to that obtained at ν_{rot} = 30 kHz, particularly near the baseline, indicating that the temperature is not constant across the sample at higher spinning frequencies. In their ^{207}Pb NMR investigation of $Pb(NO_3)_2$, van Gorkom and coworkers found that for samples spinning at 12 kHz in 4 mm

zirconia rotors, the temperature in the upper and lower regions of the probe differed by 5 K from that found at the center of the rotor. This was attributed to the bearing gas, which flows over these regions of the rotor.[11] Certainly the narrower ^{207}Pb NMR line widths for MAS samples of lead nitrate[13,18-24] compared to those for $MAPbCl_3$ render the former more suitable for the measurement of temperature gradients under MAS conditions.

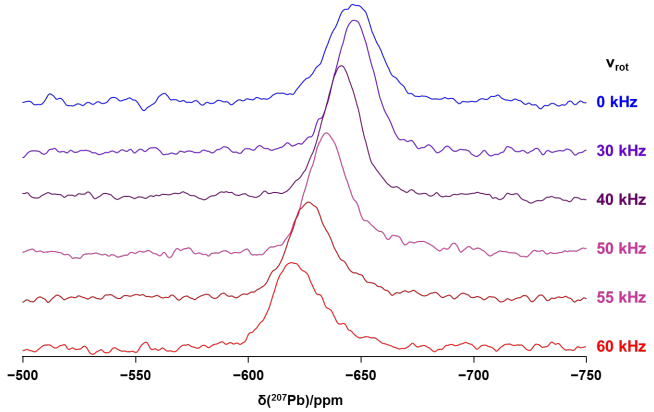

Figure 5. ^{207}Pb NMR spectra of $MAPbCl_3$ packed in a 1.3 mm outer diameter rotor obtained at 21.1 T at room temperature with the indicated spinning frequencies. Spectra are plotted with the relative intensities as obtained experimentally.

Chemical Shift Reference

In general, chemical shifts for solid-state NMR spectra are referenced via secondary reference samples for a given nucleus.[54] For example, the primary reference sample for ^{207}Pb NMR spectroscopy is $Pb(CH_3)_4$,[22,54] but generally secondary references are used due to serious concerns about the toxicity of this compound.[55] A common secondary standard for ^{207}Pb NMR measurements has been $Pb(NO_3)_2$, either as a solid[56] or in solution.[57] Unfortunately, the factors that make ^{207}Pb an ideal nucleus for NMR thermometry, its high sensitivity to temperature,[22] render it unsuitable as a secondary shift reference. In addition, ^{207}Pb NMR spectroscopy of non-spinning solid samples of $Pb(NO_3)_2$ yields a broad asymmetric ^{207}Pb NMR powder pattern,[56]

reducing the accuracy of the isotropic chemical shift. MAS reduces the breadth of the anisotropic powder pattern to an isotropic peak and some spinning side bands (depending on the spinning frequency and magnetic field strength). At typical spectrometer frequencies, the isotropic peak is usually symmetric and sharp, although frictional heating may affect its position and if this heating is non-uniform, the resulting peak may be asymmetric.[11]

To avoid difficulties in referencing ^{207}Pb NMR spectra as outlined above, some researchers have chosen to use the frequency ratio method,[58] whereby the ^{207}Pb chemical shift of $Pb(CH_3)_4$ (neat) is set to 20.920599 % of that for the ^{1}H frequency of TMS.[54] Unfortunately, the latter is also sensitive to concentration[59] and slightly to temperature.[56,60–62] The dilute TMS typically used as a primary ^{1}H reference renders it impractical for lower-sensitivity solid-state NMR probes. As discussed in the supporting information, DSS serves as a suitable alternative to TMS for referencing via the frequency ratio method and in fact was used for our initial calibration (see SI).

In their 2001 IUPAC recommendations, Harris *et al*. encouraged the use of internal referencing when practical.[54] This rarely is the case when dealing with solid samples, but as seen in Fig. 6, the ^{13}C and ^{1}H NMR spectra for MAS samples of $MAPbCl_3$ yield relatively narrow peaks, with full width at half maximum (FWHM) of 16 Hz for ^{13}C and 200 to 270 Hz for ^{1}H, ideal for use as internal references; these spectra were obtained in 84 and 4 mins, respectively, but spectra with adequate signal/noise for referencing may be obtained with a single transient for ^{1}H (1 min) or 4 transients for ^{13}C (4 min). Thus, this approach quickly provides the data needed for referencing, although spectroscopists may find the long recycle delays required for ^{1}H or ^{13}C CP NMR for this sample inconvenient if further setup (such as shimming) is required. As seen in Fig. 6B, even in the absence of spinning, the ^{13}C peak (FWHM = 700 Hz) may be used for

referencing despite the much greater breadth, although in this case a minimum of 30 minutes would be required to obtain a spectrum with an adequate signal/noise ratio. As for the ^{1}H nuclei of DSS, used for chemical shift calibration, the chemical shifts of these nuclei show no significant variation with temperature (*vide infra*). By obtaining ^{1}H spectra for DSS (see SI) the 100 % ^{1}H reference frequency was determined and thus modified frequency ratios, $\Xi^{X}(^{207}Pb)$, where X defines the sample used for the frequency ratio, were derived as summarized in Table 2. Note that by determining the frequency of either peak shown in Fig. 6, application of the appropriate frequency ratio listed in Table 2 will yield the identical reference frequency for ^{207}Pb (*i.e.*, that for $Pb(CH_3)_4$). If using an MAS probe capable of ^{1}H acquisition, referencing *via* ^{1}H of $MAPbCl_3$ offers an additional benefit: the magnet stability may be monitored during data acquisition to ensure that changes in ^{207}Pb peak positions are properly ascribed to a temperature effect rather than external factors, such as magnet drift. This may be particularly useful for spectroscopists using mature magnets or ultrahigh magnetic fields, since solid-state NMR magnets are not frequency-locked and changes in chemical shifts due to magnet drift may mask the temperature effect on chemical shifts. Finally, it is important to note that, since the goal of this step is to indirectly determine the ^{207}Pb frequency of the reference standard, $Pb(CH_3)_4$ at room temperature, the ^{1}H or ^{13}C data should be obtained at or near room temperature.

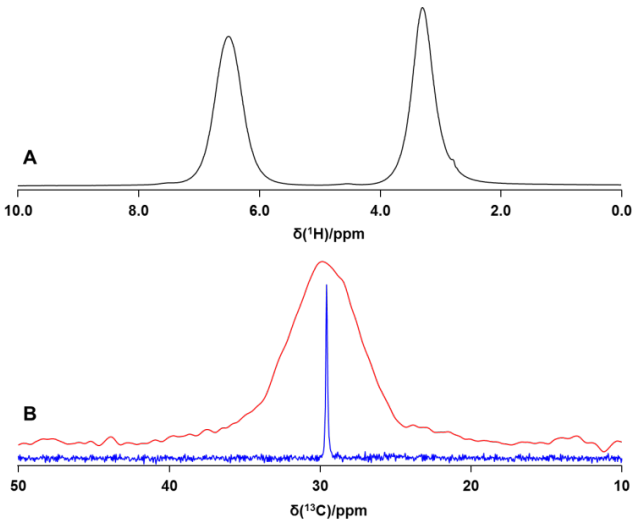

Figure 6. ^{1}H (A) and ^{13}C (B) NMR spectra of $MAPbCl_3$, acquired at 11.75 T at ambient temperature (not corrected for frictional heating). The ^{1}H NMR spectrum was acquired at a spinning frequency of 12 kHz (4 transients co-added) while the ^{13}C NMR spectra were acquired at a spinning frequency of 3.0 kHz (lower, blue trace; 84 transients co-added) or under non-spinning conditions (middle, red trace; 252 transients co-added).

Table 2. Frequency Ratios to Determine ν_{ref} for $Pb(CH_3)_4$.[a]

Nucleus	$\Xi^X(^{207}Pb)$/%	
	X	Ratio
^{1}H	DSS	20.920599
^{1}H	NH_3	20.920463
^{1}H	CH_3	20.920530
^{13}C	CH_3	83.197311

a. The frequency ratio given here for the methyl ^{1}H of DSS was obtained from reference 54. Other values given here were derived from this value or the corresponding value for ^{13}C of TMS, also given in reference 54. See Supporting Information for details of the procedure.

We have developed an alternative method for measuring sample temperature that does not involve measuring the ^{207}Pb chemical shift of $MAPbCl_3$. By knowing the "exact" resonance

frequency ratio, $\nu(^{207}\mathrm{Pb})/\nu(^{13}\mathrm{C})$ at one temperature, and knowing that $\partial\sigma(^{207}\mathrm{Pb})/\partial\mathrm{T} = -0.905 \pm 0.010$ ppm·K^{-1} (previous section), one can easily derive the following equation,

$$\mathrm{T/K} = \left\{1.0000000 - 0.831\,436\,02\left[\frac{\nu(^{13}\mathrm{C})}{\nu\left(^{207}\mathrm{Pb(T)}\right)}\right]\right\}(1.105 \times 10^6) + 291.3 \qquad 3$$

Equation 3 was derived from the frequency ratio, $\nu(^{13}\mathrm{C})/\nu(^{207}\mathrm{Pb(T)})$ that we measured numerous times for $MAPbCl_3$ at 291.3 ± 0.5 K; see SI for more details. The advantage of using this approach is that one does not have to be concerned with bulk magnetic susceptibility effects.[63–67]

Similarly, one can determine the temperature from the ratio of the methyl proton nuclei, $\nu(^{1}\mathrm{H})$, to the lead-207 frequency, $\nu(^{207}\mathrm{Pb}(T))$, using Equation 4,

$$\mathrm{T/K} = \left\{1.0000000 - 0.209\,070\,25\left[\frac{\nu(^{1}\mathrm{H})}{\nu\left(^{207}\mathrm{Pb(T)}\right)}\right]\right\}(1.105 \times 10^6) + 291.3 \qquad 4$$

We recommend that one uses the $-CH_3$ ^{1}H nuclei as opposed to the $-NH_3$ ^{1}H nuclei as the methyl resonance is narrower.

We have tested Equations 3 and 4 over the temperature range 177 to 378 K and find excellent agreement (± 0.5 K) with values determined using the methanol, ethylene glycol, a thermocouple and Equation 2. The main assumption in deriving Equation 3 is that $\partial\nu(^{13}\mathrm{C})/\partial\mathrm{T}$ is negligible compared to $\partial\nu(^{207}\mathrm{Pb})/\partial\mathrm{T}$. This was confirmed at temperatures near ambient in our lab since ^{13}C chemical shifts did not noticeably change with large changes in the MAS frequency, although the temperature of the sample increases significantly under these conditions (see Fig. 4). Likewise, in their investigation of a related compound, Baikie *et al.*[47] found that the ^{13}C chemical shift dependence of $MAPbI_3$, which undergoes a phase transition at ≈333 K, is approximately 0.01 ppm/K. Thus we recommend that the initial calibration be undertaken at 293 ±10 K. Once the initial temperature has been determined, values at other temperatures may be

determined from the chemical shift dependence (0.905 ppm/K) for ^{207}Pb chemical shift of $MAPbCl_3$. Similarly, it is assumed that $\partial\nu(^1H)/\partial T$ is negligible (confirmed as described above for ^{13}C) compared to $\partial\nu(^{207}Pb)/\partial T$ in deriving Equation 4.

^{207}Pb – A New Standard

Besides its use as a temperature calibration standard, $MAPbCl_3$ may also serve as the standard for pulse calibration. As outlined in the previous section, the properties of the ^{1}H and ^{13}C nuclei of $MAPbCl_3$ (sharp peaks, insensitivity to temperature) make these ideal for referencing ^{207}Pb chemical shifts *via* the frequency ratio method. Thus, $MAPbCl_3$ is an ideal standard sample to setup for solid-state ^{207}Pb NMR experiments.

Conclusions

An NMR investigation of the temperature dependence of the ^{207}Pb chemical shifts for $MAPbCl_3$ has been undertaken. ^{207}Pb NMR spectra of the sample were acquired at several fields, ranging from 7.05 to 21.1 T (*i.e.*, 300 to 900 MHz for ^{1}H), at MAS frequencies ranging from 0 to 60 kHz, in rotors with outer diameters ranging from 1.3 to 7.0 mm. Because of short ^{207}Pb T_1 relaxation times (1.5(1) s at 293 K at 9.4 T), temperature calibration spectra can be acquired in a few minutes. The sample offers significant advantages for NMR thermometry: (i) The ^{207}Pb NMR chemical shifts are highly sensitive to temperature, 0.905 ± 0.010 ppm·K^{-1}, approximately 20 % greater than the value for $Pb(NO_3)_2$, 0.758 ppm·K^{-1}.[11,16–22] (ii) It is stable in its cubic phase over a wide temperature range, from 178 to approximately 450 K.[42] (iii) The response to temperature is linear ($R^2 = 0.9996$). (iv) Because the ^{207}Pb nuclei are in octahedral environments when the sample is in its cubic phase, at $\mathbf{B}_0 \geq 7.05$ T, symmetric ^{207}Pb NMR peaks are obtained for non-spinning samples, avoiding complications obtained when calibrating the temperature

with a sample that yields asymmetric peaks, and (v) the sharp ^{1}H and ^{13}C NMR peaks allow the calibration of the chemical shift scale based on the spectra of temperature-insensitive nuclei using an internal reference. By following the protocols outlined in this study, the temperature of the sample within an NMR magnet can be determined with an uncertainty estimated to be $\leq \pm 2$ K.

Besides providing the NMR community with a new more sensitive sample for NMR thermometry, this study serves to remind spectroscopists that significant errors in reported temperatures can occur if set temperatures are not calibrated with a suitable NMR temperature standard. In addition, the effects of frictional heating have been investigated.

Supporting Information Available: Summary of NMR thermometers; summary of experimental parameters; additional chemical shift vs temperature plots; ^{207}Pb spectra of $MAPbCl_3$ and DSS; description of the frequency ratio method as applied here.

Acknowledgements

The authors acknowledge funding support from the Natural Sciences and Engineering Research Council (NSERC) of Canada (DG no. 05447-2016). Access to the 21.1 T NMR spectrometer was provided by the National Ultrahigh-Field NMR Facility for Solids (Ottawa, Canada), a national research facility funded by a consortium of Canadian Universities, supported by the National Research Council of Canada and Bruker BioSpin, and managed by the University of Ottawa (http://nmr900.ca); we thank Dr. Victor V. Terskikh for obtaining spectra on this instrument. The University of Alberta is thanked for research support (VKM) and an internship (AG) through the University of Alberta Research Experience (UARE) program. Finally,

members of the Michaelis Research Group as well as Mr. Abdelrahman Askar are thanked for valuable discussions.

References

[1] Palmer III, A.G. A Dynamic Look Backward and Forward. *J. Magn. Reson*. **2016**, *266*, 73−80.

[2] Kozlova, S.G.; Sergeev, N.A.; Buznik, V.M. Gabuda's Model of Averaging Local Magnetic Fields in Solid-State NMR. The Mobility of Atoms and Molecules. *J. Struct. Chem*. **2016**, 57, 213−237.

[3] Hansen, S.K.; Bertelsen, K.; Paaske, B.; Nielsen, N.C.; Vosegaard, T. Solid-State NMR Methods for Oriented Membrane Proteins. *Prog. Nucl. Magn. Reson. Spectrosc*. **2015**, *88−89*, 48−85.

[4] Polenova, T.; Gupta, R.; Goldbourt, A. Magic Angle Spinning NMR Spectroscopy: A Versatile Technique for Structural and Dynamic Analysis of Solid-Phase Systems. *Anal. Chem*. **2015**, *87*, 5458−5469.

[5] Zheng, G.; Price, W.S. Simultaneous Convection Compensation and Solvent Suppression in Biomolecular NMR Diffusion Experiments. *J. Biomol. NMR* **2009**, *45*, 295−299.

[6] Webb, A.G. Advances in Probe Design for Protein NMR. *Annu. Rep. NMR Spectrosc.* **2006**, *58*, 1−50.

[7] Koptyug, I.V. Magnetic Resonance Imaging Methods in Heterogeneous Catalysis. *Spectrsoc. Prop. Inorg. Organomet. Compd.* **2014**, *45*, 1−42.

[8] Kovacs, H.; Moskau, D.; Spraul, M. Cryogenically Cooled Probes—a Leap in NMR Technology. *Progress Nucl. Magn. Reson. Spectrosc.* **2005**, *46*, 131−155.

[9] McNeill, S.A.; Gor'kov, P.L.; Struppe, J.; Brey, W.W.; Long, J.R. Optimizing ssNMR Experiments for Dilute Proteins in Heterogeneous Mixtures at High Magnetic Fields. *Magn. Reson. Chem.* **2007**, *45*, S209−S220.

[10] Stringer, J.A.; Bronimann, C.E.; Mullen, C.G.; Zhou, D.H.; Stellfox, S.A.; Li, Y.; Williams, E.H.; Rienstra, C.M. Reduction of RF-Induced Sample Heating with a Scroll Coil Resonator Structure for Solid-State NMR Probes. *J. Magn. Reson.* **2005**, *173*, 40−48.

[11] van Gorkom, L.C.M.; Hook, J.M.; Logan, M.B.; Hanna, J.V.; Wasylishen, R.E. Solid-State Lead-207 NMR of Lead(II) Nitrate: Localized Heating Effects at High Magic Angle Spinning Speeds. *Magn. Reson. Chem*. **1995**, *33*, 791−795.

[12] Demers, J.-P.; Chevelkov, V.; Lange, A. Progress in Correlation Spectroscopy at Ultra-fast Magic-Angle Spinning: Basic Building Blocks and Complex Experiments for the Study of Protein Structure and Dynamics. *Solid State Nucl. Magn. Reson.* **2011**, *40*, 101−113.

[13] Haw, J.F. Thermometry. In *Encyclopedia of NMR*. Harris, R. K.; Wasylishen. R. E., Eds. John Wiley & Sons: Chichester, 2012; Vol. 9, pp 5079−5082. DOI: 10.1002/9780470034590.emrstm0561. Posted online 14th January, 2009.

[14] Raiford, D.S.; Fisk, C.L.; Becker, E.D. Calibration of Methanol and Ethylene Glycol Nuclear Magnetic Resonance Thermometers. *Anal. Chem*. **1979**, *51*, 2050−2051.

[15] Tsitovich, P.B.; Cox, J.M.; Benedict, J.B.; Morrow, J.R. Six-Coordinate Iron(II) and Cobalt(II) ParaSHIFT Agents for Measuring Temperature by Magnetic Resonance Spectroscopy. *Inorg. Chem*. **2016**, *55*, 700−716.

[16] Kemp, T.F.; Balakrishnan, G.; Pike, K.J.; Smith, M.E. Dupree, R. Thermometers for Low Temperature Magic Angle Spinning NMR. *J. Magn. Reson*. **2010**, *204*, 169−172.

[17] Mildner, T.; Ernst, H.; Freude, D. ^{207}Pb NMR Detection of Spinning-Induced Temperature Gradients in MAS Rotors. *Solid State Nucl. Magn. Reson*. **1995**, *5*, 269−271.

[18] Beckmann, P.A.; Dybowski, C. A Thermometer for Nonspinning Solid-State NMR Spectroscopy. *J. Magn. Reson*. **2000**, *146*, 379−380.

[19] Takahashi, T.; Hawashima, H.; Sugisawa, H.; Baba, T. ^{207}Pb Chemical Shift Thermometer at High Temperature for Magic Angle Spinning Experiments. *Solid State Nucl. Magn. Reson*. **1999**, *15*, 119−123.

[20] Guan, X.; Stark, R.E. A General Protocol for Temperature Calibration of MAS NMR Probes at Arbitrary Spinning Speeds. *Solid State Nucl. Magn. Reson*. **2010**, *38*, 74−76.

[21] Bielecki, A.; Burum, D.P. Temperature Dependence of ^{207}Pb MAS Spectra of Solid Lead Nitrate. An Accurate Sensitive Thermometer for Variable-Temperature MAS. *J. Magn. Reson. Ser. A,* **1995**, *116*, 215−220.

[22] Dybowski, C.; Neue, G. Solid State ^{207}Pb NMR Spectroscopy. *Prog. Nucl. Magn. Reson. Spectrosc*. **2002**, *41*, 153−170.

[23] Barnes, A.B.; Markhasin, E.; Daviso, E.; Michaelis, V.K.; Nanni, E.A.; Jawla, S.K.; Mena, E.L.; DeRocher, R.; Thakkar, A.; Woskov, P.P.; Herzfeld, J.; Temkin, R.J.; Griffin, R.G. *J. Magn. Reson*. **2012**, *224*, 1−7.

[24] Thurber, K.R.; Tycko, R. Measurement of Sample Temperatures Under Magic-Angle Spinning from the Chemical Shift and Spin-Lattice Relaxation Rate of ^{79}Br in KBr Powder. *J. Magn. Reson.* **2009**, *196*, 84−87.

[25] Sullivan, N.S. NMR at Very Low Temperatures: Population Difference Thermometry. *Bull. Magn. Reson*. **1997**, *18*, 258−264.

[26] Pan, H.; Gerstein, B.C. NMR of ^{31}P in $(VO)_2P_2O_7$ as an Internal Temperature Standard in High-Temperature NMR. *J. Magn. Reson*. **1991**, *92*, 618−619.

[27] Aliev, A.E.; Harris, K.D.M. Simple Technique for Temperature Calibration of a MAS Probe for Solid-State NMR Spectroscopy. *Magn. Reson. Chem*. **1994**, *32*, 366−369.

[28] van Wüllen, L.; Schwering, G.; Naumann, E.; Jansen, M. MAS-NMR at Very High Temperatures. *Solid State Nucl. Magn. Reson.* **2004**, *26*, 84−86.

[29] Umegawa, Y.; Tanaka, Y.; Nobuaki, M.; Murata, M. ^{13}C-TmDOTA as Versatile Thermometer Compound for Solid-State NMR of Hydrated Lipid Bilayer Membranes. *Magn. Reson. Chem*. **2016**, *54*, 227−233.

[30] Riddell, F.G.; Spark, R.A.; Günther, G.V. Measurement of Temperature in ^{13}C CP/MAS NMR. *Magn. Reson. Chem.* **1996**, 34, 824−828.

[31] Wu, J.; Kim, N.; Stebbins, J.F. Temperature Calibration for High-Temperature MAS NMR to 913 K: ^{63}Cu MAS NMR of CuBr and CuI, and ^{23}Na MAS NMR of $NaNbO_3$. *Solid State Nucl. Magn. Reson.* **2011**, *40*, 45−50.

[32] Purusottam, R.N.; Bodenhausen, G.; Tekely, P. Determination of Sample Temperature in Unstable Static Fields by Combining Solid-State ^{79}Br and ^{13}C NMR. *J. Magn. Reson.* **2014**, *246*, 69−71.

[33] Grimmer, A.-R.; Kretschmer, A.; Cajipe, V.B. Influence of Magic Angle Spinning on Sample Temperature. *Magn. Reson. Chem.* **1997**, *35*, 86−90.

[34] Grey, C.P.; Cheetham, A.K.; Dobson, C.M. Temperature-Dependent Solid-State ^{119}Sn MAS NMR of $Nd_2Sn_2O_7$, $Sm_2Sn_2O_7$, and $Y_{1.8}Sm_{0.2}O_7$. Three Sensitive Chemical Shift Thermometers. *J. Magn. Reson. A*, **1993**, *101*, 299−306.

[35] Langer, B.; Schnell, I.; Speiss, H.W.; Grimmer, A.-R. Temperature Calibration under Ultrafast MAS Conditions. *J. Magn. Reson.* **1999**, *138*, 182−186.

[36] Sarkar, R.; Concistrè, M.; Johannessen, O.G.; Beckett, P.; Denning, M.; Carravetta, M.; al-Mosawi, M.; Beduz, C.; Yang, Y.; Levitt, M.H. An NMR Thermometer for Cryogenic Magic-Angle Spinning NMR: The Spin-Lattice Relaxation of ^{127}I in Cesium Iodide. *J. Magn. Reson.* **2011**, *212*, 460−463.

[37] Beckett, P.; Denning, M.S.; Carravetta, M.; Kalda, A.; Heinmaa, I. Field Dependence of the Relaxation of ^{79}Br in KBr and its use as a Temperature Calibrant. *J. Magn. Reson.* **2012**, *223*, 61−63.

[38] Wasylishen, R.E.; Knop, O.; Macdonald, J.B. Cation Rotation in Methylammonium Lead Halides. *Solid State Commun*. **1985**, *56*, 581−582.

[39] Knop, O.; Wasylishen, R.E.; White, M.A.; Cameron, T.S.; Van Oort, M.J.M. Alkylammonium Lead Halides. Part. 2. $CH_3NH_3PbX_3$ (X = Cl, Br, I) Perovskites: Cuboctahedral Halide Cages with Isotropic Cation Reorientation. *Can. J. Chem*. **1990**, *68*, 412−422.

[40] Askar, A.M.; Bernard, G.M.; Wilstshire, B.; Shankar, K.; Michaelis, V.K. Multinuclear Magnetic Resonance Tracking of Hydro, Thermal, and Hydrothermal Decomposition of $CH_3NH_3PbI_3$. *J. Phys. Chem. C*, **2017**, *121*, 1013−1024.

[41] Onoda-Yamamuro, N.; Matsuo, T.; Suga, H. Calorimetric and IR Spectroscopic Studies of Phase Transitions in Methylammonium Trihalogenoplumbates (II). *J. Phys. Chem. Solids*, **1990**, *51*, 1383−1395.

[42] Brunetti, B.; Cavallo, C.; Ciccioli A.; Gigli, G.; Latini, A. On the Thermal and Thermodynamic (In)stability of Methylammonium Lead Halide Perovskites. *Sci. Rep*. **2016**, 6, 31896.

[43] Poglitsch, A.; Weber, D. Dynamic Disorder in Methylammoniumtrihalogenoplumbates (II) Observed by Millimeter-Wave Spectroscopy. *J. Chem. Phys*. **1987**, *87*, 6373−6378.

[44] Xu, Q.; Eguchi, T.; Nakayama, H.; Nakamura, N.; Kishita, M. Molecular Motions and Phase Transitions in Solid $CH_3NH_3PbX_3$ (X = Cl, Br, I) as Studied by NMR and NQR. *Z. Naturforsch*. **1991**, *46a*, 240−246.

[45] Maalej, A.; Abid, Y.; Kallel, A.; Daoud, A.; Lautié, A.; Romain, F. Phase Transitions and Crystal Dynamics in the Cubic Perovskite $CH_3NH_3PbCl_3$. *Solid State Comm*. **1997**, *103*, 279−284.

[46] Chi, L.; Swainson, I.; Cranswick, L.; Her, J.-H.; Stephens, P.; Knop, O. The Ordered Phase of Methylammonium Lead Chloride $CH_3ND_3PbCl_3$. *J. Solid State Chem*. **2005**, *178*, 1376−1385.

[47] Baikie, T.; Barrow, N.S.; Fang, Y.; Keenan, P.J.; Slater, P.R.; Piltz, R.O.; Gutmann, M.; Mhaisalkar, S.G.; White, T.J. A Combined Single Crystal Neutron/X-ray Diffraction and Solid-State Nuclear Magnetic Resonance Study of the Hybrid Perovskites $CH_3NH_3PbX_3$ (X = I, Br and Cl). *J. Mat. Chem. A*, **2015**, *3*, 9298−9307.

[48] Altounian, N.; Glatfelter, A.; Bai, S.; Dybowski, C. Thermodynamics of Ion Pairing in Lead Nitrate Solutions as Determined with ^{207}Pb NMR Spectroscopy. *J. Phys. Chem. B*, **2000**, *104*, 4723−4725.

[49] Lutz, O.; Stricker, G. The Magnetic Moment of ^{207}Pb and the Shielding of Lead Ions by Water. *Phys. Lett*. **1971**, *35A*, 397−398.

[50] Weber, D. $CH_3NH_3PbX_3$, ein Pb(II)-System mit Kubischer Perowskitstruktur. *Z. Naturforsch*. **1978**, *33b*, 1443−1445.

[51] Eichele, K. WSolids NMR Simulation Package, Version 1.21.3; Universität Tübingen: Tübingen, Germany, 2015, http://anorganik.uni-tuebingen.de/klaus/soft/index.php. Early versions of this software were prepared in REW's lab in the late 1980's and the 1990's.

[52] Marat, K. SpinWorks, Version 3.1.7.0; University of Manitoba, Canada, 2010, https://home.cc.umanitoba.ca/~wolowiec/spinworks/.

[53] Harris, R.K.; Olivieri, A.C. Quadrupolar Effects Transferred to Spin-½ Magic-Angle Spinning Spectra of Solids. *Prog. Nucl. Magn. Reson. Spectrosc.* **1992**, *24*, 435−456.

[54] Harris, R.K.; Becker, E.D.; Cabral de Menezes, S.M.; Goodfellow, R.; Granger, P. NMR Nomenclature. Nuclear Spin Properties and Conventions for Chemical Shifts. *Pure Appl. Chem.* **2001**, *73*, 1795−1818.

[55] Patočka, J. Organic Lead Toxicology. *Acta Med.* **2008**, *51*, 209−213.

[56] Neue, G.; Dybowski, C.; Smith, M.L.; Hepp, M.A.; Perry, D.L. Determination of $^{207}Pb^{2+}$ Chemical Shift Tensors from Precise Powder Lineshape Analysis. *Solid State Nucl. Magn. Reson.* **1996**, *6*, 241−250.

[57] Maciel, G.E.; Dallas, J.L. ^{207}Pb Pulse Fourier Transform Nuclear Magnetic Resonance. A Promising New Tool for Studies in Lead Chemistry. *J. Am. Chem. Soc.* **1973**, *95*, 3039−3040.

[58] Wrackmeyer, B.; Horchler, K. ^{207}Pb-NMR Parameters. *Ann. Rep. NMR Spectrosc.* **1990**, *22*, 249−306.

[59] Bacon, M.R.; Maciel, G.E. Solvent Effects on the Five Shielding Constants in Tetramethylsilane and Cyclohexane. *J. Am. Chem. Soc.* **1973**, *95*, 2413−2426.

[60] Jameson, C.J.; Jameson, A.K.; Cohen, S.M. Absolute Temperature Dependence of Chemical Shielding of Some Reference Nuclei. *J. Magn. Reson.* **1975**, *19*, 385−392.

[61] Harris, R.K.; Becker, E.D.; Cabral De Menezes, S.M.; Granger, P.; Hoffman, R.E.; Zilm, K.W. Further Conventions for NMR Shielding and Chemical Shifts (IUPAC Recommendations 2008). *Pure Appl. Chem.* **2008**, *80*, 59−84.

[62] Hoffman, R.E.; Becker, E.D. Temperature Dependence of the ^{1}H Chemical Shift of Tetramethylsilane in Chloroform, Methanol, and Dimethylsulfoxide. *J. Magn. Reson.* **2005**, *176*, 87−98.

[63] Dickinson, W.C. The Time Average Magnetic Field at the Nucleus in Nuclear Magnetic Resonance Experiments. *Phys. Rev.* **1951**, *81*, 717−731.

[64] Live, D.H.; Chan, S.I. Bulk Susceptibility Corrections in Nuclear Magnetic Resonance Experiments Using Superconducting Solenoids. *Anal. Chem.* **1970**, *42*, 791−792.

[65] Hoffman, R.E. Measurement of Magnetic Susceptibility and Calculation of Shape Factor of NMR Samples. *J. Magn. Reson.* **2006**, *178*, 237−247.

[66] Morcombe, C.R.; Zilm, K.W. Chemical Shift Referencing in MAS Solid State NMR. *J. Magn. Reson.* **2003**, *162*, 479−486.

[67] Garroway, A.N. Magic-Angle Spinning of Liquids. *J. Magn. Reson.* **1982**, *49*, 168−171.